Journal of Alloys and Compounds 489 (2010) 91–98

Contents lists available at ScienceDirect

Journal of Alloys and Compounds

journal homepage: www.elsevier.com/locate/jallcom

Synthesis of nanocrystalline Cd–Zn ferrite by ball milling and its stability at elevated temperatures

M. Sinha, S.K. Pradhan*

Department of Physics, The University of Burdwan, Golapbag, Burdwan 713104, West Bengal, India

ARTICLE INFO

Article history:
Received 3 February 2009
Accepted 7 September 2009
Available online 11 September 2009

Keywords:
Nanocrystalline $(Zn,Cd)Fe_2O_4$
Ball milling
Microstructure characterization
Annealing
Phase stability

ABSTRACT

High energy ball milling of stoichiometric (0.5:0.5:1 mole fraction) mixture of CdO, ZnO and α-Fe_2O_3 powders in air at room temperature results in formation of a non-stoichiometric Zn-rich $(Zn,Cd)Fe_2O_4$ phase with normal spinel structure having tetrahedral vacancies. The ferrite phase is initiated at 1 h of milling and after 25 h milling, 0.96 mole fraction of ferrite is formed and 0.04 mole fraction of CdO phase remained unreacted. The phase stability study of nanocrystalline non-stoichiometric $(Zn,Cd)Fe_2O_4$ powder annealed at elevated temperatures reveals that the Zn-rich ferrite phase remained stable up to 973 K and then slowly transformed towards Cd-rich $(Cd,Zn)Fe_2O_4$ phase following the release of divalent cations from ferrite lattice of normal spinel structure. The non-stoichiometric ferrite phase with almost similar composition has also been obtained by conventional ceramic route by sintering the same stoichiometric mixture at 973 K for 1 h. Microstructure characterization in terms of several lattice imperfections, relative phase abundances, cation distribution, and phase stability studies of unmilled, ball-milled and annealed samples is made by employing the Rietveld's structure refinement methodology using X-ray powder diffraction data. The analysis reveals that the particle size of ferrite phase reduces to ~7 nm after 25 h of milling and after annealing at 1273 K for 1 h it grows up to ~700 nm. However, in case of ferrite prepared by ceramic route it grows up to ~250 nm which is quite less than the annealed ball-milled samples.

1. Introduction

In recent years the synthesis of nanocrystalline magnetic materials has been investigated intensively due to their unique and novel properties and wide variety of potential applications in high density magnetic recording, color imaging, microwave devices, bioprocessing, magnetic refrigeration and magneto-optical devices [1–3]. Magnetic nanocrystalline materials also hold great promise for atomic engineering of materials with functional magnetic properties [4–6]. Among several magnetic materials spinel ferrites are very important magnetic materials and are very much sensitive to manufacturing process.

Many synthetic roots have been employed to prepare ferrite nanocrystals [7–9]. High energy ball milling is one of the 'top-down' processing technique for nanocrystalline ferrite powder, exhibiting new and unusual properties [10–13]. Zinc ferrite prepared by conventional ceramic method belongs to normal spinel structure with Zn^{2+} in the tetrahedral and Fe^{3+} in the octahedral sites of a cubic close packing of oxygen atoms of $ZnFe_2O_4$ [13–16] lattice. For practical use of nanocrystalline ferrites in different applications they need to be shaped according to requirements and sintered at elevated temperatures. From the application point of view, it is therefore essential to study the phase stability and changes in microstructure after the heat treatment of nanocrystalline materials. We have reported that nanocrystalline zinc ferrite synthesized at room temperature by high energy ball milling formed with a metastable inverse spinel structure and after annealing at elevated temperatures it converted completely to the normal spinel structure [17]. In our recent study [18], we have reported the detailed microstructure characterization of nanocrystalline Mg–Zn ferrite powders prepared by ball milling the stoichiometric mixture of MgO, ZnO and α-Fe_2O_3 powders at room temperature and the stability of nanoferrite phase at elevated temperatures [19]. In our present study (i) we have synthesized nanocrystalline Cd–Zn ferrite by ball milling the stoichiometric mixture of CdO, ZnO, and α-Fe_2O_3 powders in a high energy planetary ball mill and studied the phase transformation kinetics and characterized the microstructure in detail in terms of several lattice imperfections and (ii) we have also sintered the unmilled mixture and annealed the 8 h and 20 h ball-milled samples to study the phase transformation kinetics and phase stability of ferrite phase at elevated temperatures. The Rietveld's analysis based on structure and microstructure refinement method [20–24] has been employed which is considered to be the best method for microstructure characterization and quantitative estimations of multiphase nanocrystalline material containing several number of overlapping reflections. To the best of our knowl-

* Corresponding author. Tel.: +91 342 2657800; fax: +91 342 2657800.
E-mail address: skp_bu@yahoo.com (S.K. Pradhan).

0925-8388/$ – see front matter © 2009 Elsevier B.V. All rights reserved.
doi:10.1016/j.jallcom.2009.09.019

Table 1
Microstructure parameters of unmilled and ball-milled CdO, ZnO and α-Fe_2O_3 powder mixture as revealed from Rietveld's analysis of XRD data.

Milling time	Phases present	Mole fraction	Lattice parameter		Particle	Size (nm)
			a (nm)	*c* (nm)		
0 h	α-Fe_2O_3	0.4951	0.5031	1.3734	59.37	0.53
	CdO	0.2377	0.4691		230.77	0.61
	ZnO	0.2672	0.3247	0.5200	193.59	1.34
1 h	α-Fe_2O_3	0.3790	0.5044	1.3747	32.12	8.58
	CdO	0.1545	0.4668		7.92	10.66
	ZnO	0.0879	0.3242	0.5188	50.00	0.80
	(Zn,Cd)Fe_2O_4	0.3786	0.8590		3.94	107.10
3 h	α-Fe_2O_3	0.1953	0.5067	1.3638	37.31	21.74
	CdO	0.1229	0.4638		2.71	10.00
	ZnO	0.0082	0.3189	0.5375	50.00	0.80
	(Zn,Cd)Fe_2O_4	0.6734	0.8492		3.99	0.08
5 h	α-Fe_2O_3	0.0909	0.5103	1.3609	38.24	14.59
	CdO	0.1075	0.4669		4.91	10.75
	ZnO	0.0092	0.3219	0.5247	50.00	0.80
	(Zn,Cd)Fe_2O_4	0.7924	0.8500		6.40	2.32
8 h	α-Fe_2O_3	0.0114	0.5036	1.3749	50.00	0.80
	CdO	0.0910	0.4670		5.98	11.35
	(Zn,Cd)Fe_2O_4	0.8976	0.8494		6.88	4.40
12 h	α-Fe_2O_3	0.0181	0.5036	1.3749	50.00	0.80
	CdO	0.0611	0.4675		6.57	13.77
	(Zn,Cd)Fe_2O_4	0.9206	0.8496		7.01	4.75
20 h	CdO	0.0393	0.4685		4.95	11.90
	(Zn,Cd)Fe_2O_4	0.9607	0.8494		7.02	5.70
25 h	CdO	0.0361	0.4684		7.17	18.3
	(Zn,Cd)Fe_2O_4	0.9639	0.8490		6.29	0.22

edge, so far the phase transformation kinetics and microstructure characterization of post-annealed nanocrystalline Cd–Zn ferrite has not been studied yet in detail by X-ray powder diffraction method.

2. Experimental

Accurately weighed starting powders of CdO (M/S Merck, 98% purity), ZnO (M/S Merck, 99% purity) and α-Fe_2O_3 (M/S Glaxo, 99% purity) taken in 0.5:0.5:1 mol.% were hand-ground by an agate mortar pestle in a doubly distilled acetone medium for more than 5 h. The dried homogeneous powder mixture was then termed as unmilled stoichiometric homogeneous powder mixture. A part of this mixture was ball-milled at room temperature in air in a planetary ball mill (Model P5, M/S Fritsch, GmbH, Germany), keeping the disk rotation speed = 300 rpm and that of the vials ~450 rpm respectively. Milling was done in hardened chrome steel vial of volume 80 ml using 30 hardened chrome steel ball of 10 mm diameter, at ball to powder mass ratio 40:1. The 8 h and 20 h ball-milled samples were annealed and unmilled (0 h) powder mixture was sintered in air at 773 K, 873 K, 973 K, 1073 K and 1273 K, each for 1 h duration in a programmable furnace.

The X-ray powder diffraction profiles of unmilled and all ball-milled and annealed samples were recorded (step size = 0.02° 2θ, counting time = 5 s, angular range = 15–80° 2θ) using Ni-filtered CuK_α radiation from a highly stabilized and automated Philips generator (PW1830) operated at 40 kV and 20 mA. The generator is coupled with a Philips X-ray powder diffractometer consisting of a PW 3710 mpd controller, PW1050/37 goniometer and a proportional counter.

3. Results and discussion

3.1. Microstructure characterization of nanocrystalline ferrite powders

The XRD powder patterns recorded from unmilled and ball-milled powder mixture of CdO, ZnO and α-Fe_2O_3 are shown in Fig. 1. The powder pattern of unmilled mixture contains only the individual reflections of ZnO, CdO and α-Fe_2O_3 phases. The intensity ratios of individual reflections are in accordance with the stoichiometric composition of the mixture. It is evident from the figure that the particle size of the starting materials reduces very fast as their peaks become broadened rapidly in the course of milling. The content of the starting phases reduces considerably after 1 h milling and particularly the ZnO phase almost vanishes after 1 h milling. However, the formation of Cd–Zn ferrite phase was not noticed clearly in the 1 h milled sample. The ferrite reflections were appeared clearly in 3 h milled sample and the content of ferrite phase increases continuously with milling time, as noticed up to 25 h of milling. The CdO phase was not used up completely in the process even after 25 h of milling, whereas the other two starting phases vanish completely

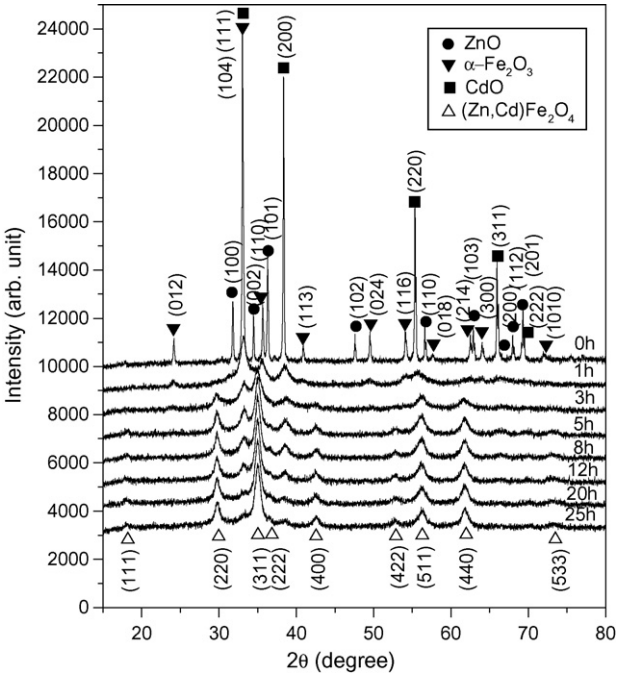

Fig. 1. (a) X-ray diffraction patterns of unmilled (0 h) and ball-milled CdO + ZnO + α-Fe_2O_3 powder mixture for different durations of ball milling.

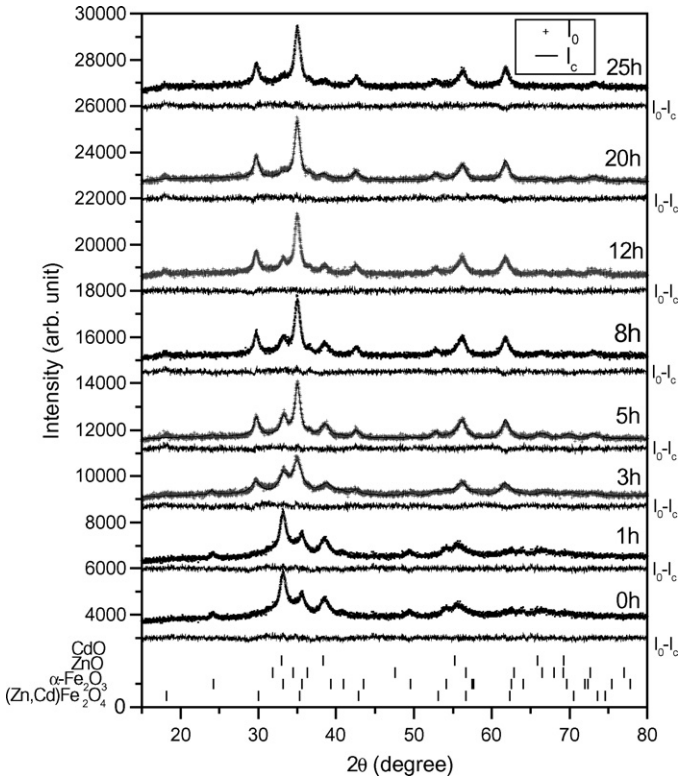

Fig. 2. Observed (+) and calculated (−) XRD patterns of unmilled (0 h) and different ball-milled samples revealed from Rietveld's powder structure refinement analysis. Residues of fittings ($I_0 - I_c$) are shown under the respective patters. Peak positions of the phases are shown at the base line.

in the course of milling. This indicates the fact that the formed ferrite phase is a non-stoichiometric in composition. There must be a number of vacancies in the tetrahedral sites of the spinel ferrite lattice due to these unreacted Cd^{2+} ions. In our previous work [18,19], we reported that Zn^{2+} ions had a marked preference for the tetrahedral sites and its presence may have reduced the chance of Cd^{2+} cation occupancy in tetrahedral sites of spinel ferrite lattice.

Fig. 2 shows the Rietveld's fitting outputs of unmilled and all ball-milled powder patterns. Peak positions of all reflections of all four phases are marked and shown at the bottom of the plot. Residual of fitting ($I_0 - I_c$) between observed (I_0) and calculated (I_c) intensities of each fitting is plotted under respective patterns. Though the XRD patterns do not show the presence of ferrite phase before 3 h milling, but the Rietveld's analysis revealed the presence of ferrite within 1 h of milling (Table 1). In case of Mg–Zn ferrite [18] we reported that initially an inverse spinel phase was formed and with increasing milling time the phase transformed to normal spinel phase. In the present analysis, all recorded XRD patterns of ball-milled samples were fitted well only with normal spinel ferrite phase. It indicates that there are tetrahedral vacancies in normal spinel structure of (Zn,Cd) ferrite which are supposed to fill with Cd^{2+} ions.

Fig. 3 shows the variation of relative phase abundances of different phases with increasing milling time. The content (mole fraction) of ZnO phase decreases very rapidly and after 3 h milling it becomes almost nil, whereas the variation of CdO content shows that initially the phase was utilized rapidly in ferrite phase but at the higher milling time, the rate of inclusion becomes very slow and till 25 h milling the phase was not completely incorporated in the ferrite matrix and ~0.04 mole fraction of the phase remained unreacted. The α-Fe_2O_3 phase content decreases in a moderate rate and after 8 h of milling a very small amount remained unutilized (Table 1). The ferrite phase content increases sharply up to 8 h of milling and then approaches towards a saturation to ~0.96 mole fraction (Table 1). It may be noticed that the ferrite content increases considerably until the α-Fe_2O_3 phase was used up completely and after that a slight increment up to 25 h milling is due to a very slow diffusion of Cd^{2+} ions into the ferrite matrix. All these variations in contents indicate that Zn^{2+} ions have occupied the tetrahedral positions quite rapidly but the Cd^{2+} ions took longer time and even after 25 h of milling some tetrahedral positions remained vacant due to insolubility of CdO in ferrite matrix. It is therefore obvious that the prepared ferrite phase is a Zn-rich non-stoichiometric (Zn,Cd)Fe_2O_4 normal spinel with tetrahedral vacancies.

The nature of variation of lattice parameter of the cubic (Zn,Cd)Fe_2O_4 phase with increasing milling time is shown in Fig. 4. It can be seen from the plot that the lattice parameter of ferrite phase formed after 1 h of milling reduces rapidly within 3 h of milling from the value 0.859 nm to ~0.849 nm (Table 1) and then remained almost invariant up to 25 h of milling. It is a well known fact that the distribution of cations among the tetrahedral and octahedral sites plays an important role in lattice parameter variation of spinel lattice [17,18,25,26]. At the primary stage of milling Cd^{2+} ions started to get into tetrahedral sites of ferrite lattice more rapidly than Zn^{2+} ions. This fact is reflected in the lattice parameter value of ferrite phase at this stage (~0.859 nm), which is close to the ICSD value of $CdFe_2O_4$ phase (0.869 nm). In the course of milling, ZnO phase utilized completely in tetrahedral vacancies but CdO phase was not and some tetrahedral sites remained unoccupied even after 25 h milling. We have reported earlier [26] that a stoichiometric Cd ferrite phase could not be obtained by ball milling the stoichiometric mixture of CdO and α-Fe_2O_3 phases. As the ZnO phase was utilized almost completely within 3 h of milling and the solubility of CdO was restricted after 3 h milling, the lattice parameter of Zn-rich ferrite phase (0.849 nm) approaches to $ZnFe_2O_4$ phase (0.844 nm) lattice parameter and the small difference may be attributed to the inclusion of Cd^{2+} in the tetrahedral vacancies.

The nature of variation of the particle size and r.m.s. lattice strain of all phases with varying milling time are shown in Fig. 5a and b respectively. Particle sizes of all phases are found to be isotropic

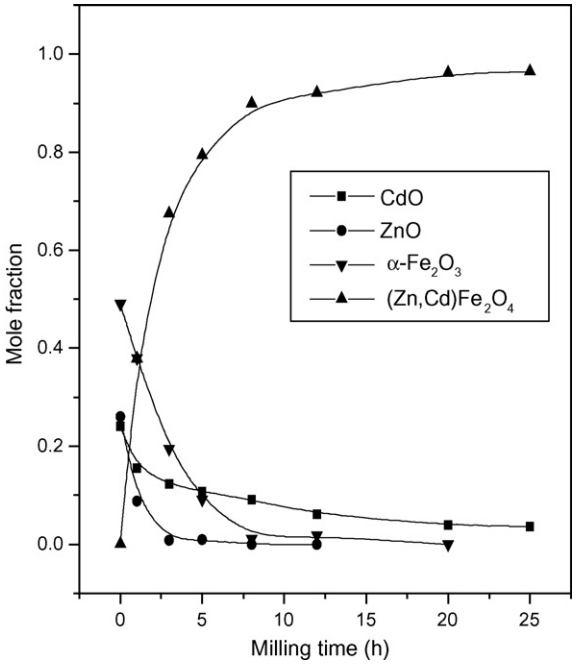

Fig. 3. Variations of mole fraction of different phases in ball-milled CdO + ZnO + α-Fe_2O_3 powder mixture with increasing milling time.

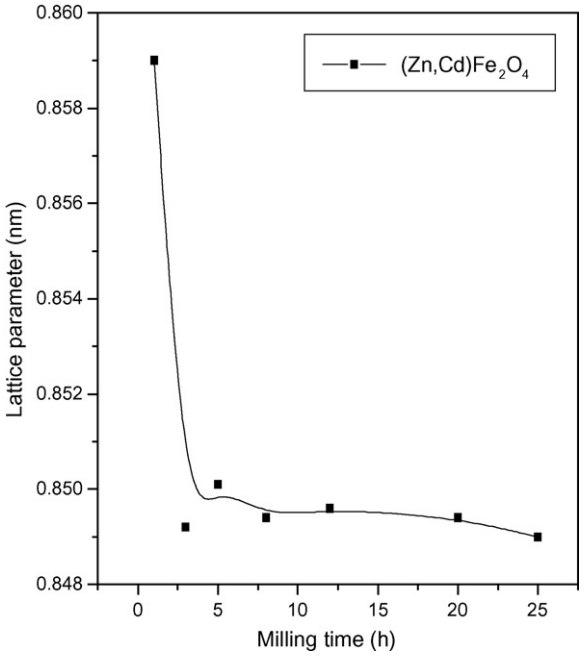

Fig. 4. Variation of lattice parameter of the (Zn,Cd)Fe_2O_4 phase with increasing milling time.

in nature. Among all the phases, CdO phase is very much prone to deformation as its particle size decreases from ~231 nm to ~8 nm within 1 h of milling (Table 1). The particle size of ZnO phase also decreases very rapidly (~193–50 nm) within 1 h of milling and after that it remains constant in higher milling times. The particle size of α-Fe_2O_3 phase shows an initial decrease below 50 nm and then increases slowly to a value ~50 nm in the course of milling. This initial reduction and then increment of the particle size value is due to the well known fracture (reduction) and re-welding (increment) process that happens usually in high energy ball milling. The ferrite phase has grown with a very small particle size (~4 nm) and increases slowly to ~7 nm after 25 h of milling.

Like particle size, the r.m.s. lattice strain of all phases are also isotropic in nature. The lattice strain of CdO phase increases very slowly with milling time and that of the ZnO phase remains unchanged. The lattice strain of the α-Fe_2O_3 phase increases rapidly up to 3 h of milling and then decreases rapidly within 8 h milling to its initial value. This particular nature of variation of lattice strain corroborates the variation in particle size of the phase. The ferrite phase grows with a very high value of lattice strain after 1 h milling and then reduces rapidly to almost zero within 5 h of milling.

3.2. Phase stability and microstructure characterization of nanocrystalline (Zn,Cd)Fe_2O_4 annealed at elevated temperatures

Fig. 6a–c shows the XRD powder patterns of the unmilled (0 h), 8 h and 20 h ball-milled samples respectively, annealed at different elevated temperatures. In Fig. 6a the ferrite phase is first noticed to form in unmilled mixture at 973 K (see inset plot). The broad (3 1 1) reflection of the phase indicates that the particle size of the newly formed ferrite phase is quite small at this stage. At higher annealing temperatures the content of the ferrite phase increases very rapidly at the expense of the starting phases. The α-Fe_2O_3 phase vanishes completely after annealing at 1273 K but the ZnO and CdO phases are still present in the sample. A strong presence of CdO phase in comparison to the ZnO phase indicates that the formed ferrite phase is a Zn-rich ferrite phase, similar to that obtained in ball mill prepared (Zn,Cd)Fe_2O_4 phase. From Fig. 6b and c it can be observed that annealing of the ball-milled samples makes the ferrite phase to decompose and both CdO and ZnO phases start to release from the ferrite matrix. The CdO phase comes out more easily than the ZnO phase. This is what expected as the Zn^{2+} ions have more affinity to tetrahedral positions than Cd^{2+} ions. Higher the ball mill period the more rapid is the decomposition rate. It can be noted from all three figures that in all annealed samples, α-Fe_2O_3 phase was completely utilized in ferrite phase formation. It indicates that the octahedral positions in normal spinel lattice are completely filled by the Fe^{3+} ions and the tetrahedral vacancies increase with increasing annealing temperatures in all ball-milled samples. It may be noted that a trace amount of $CdCO_3$ phase was also formed at the early stage of annealing (in open air) and finally decomposed into CdO and CO_2 phases.

The variation of mole fractions of all phases present in the sample with increasing annealing temperature is plotted in Fig. 7a–c for the unmilled (0 h), 8 h and 20 h ball-milled samples respectively. An observation of Fig. 7a reveals that the formation of the ferrite phase from the homogeneous powder mixture of CdO, ZnO and α-Fe_2O_3 is started at 973 K and its amount increases rapidly at higher annealing temperatures. Contents of all starting phases

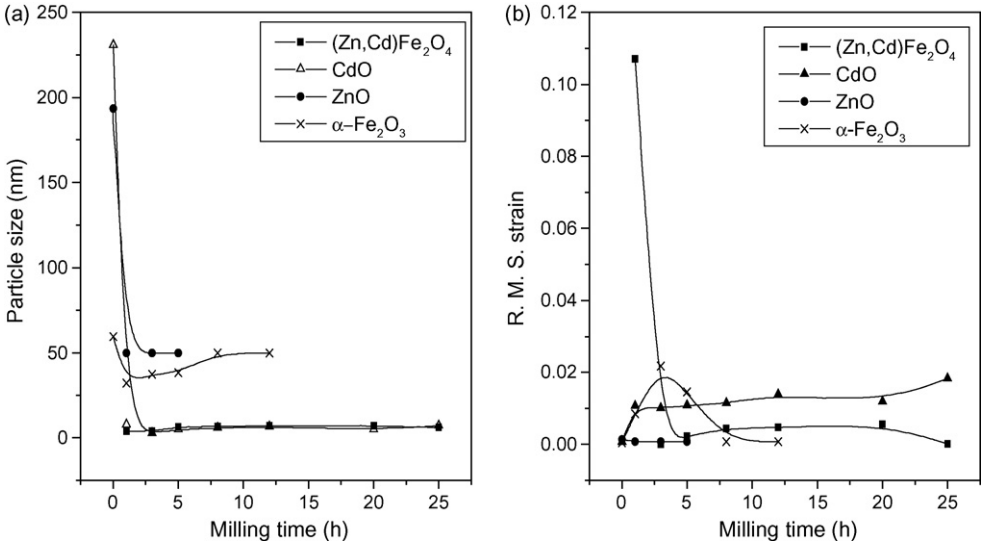

Fig. 5. Variations of (a) particle size and (b) r.m.s. lattice strain of different phases in ball-milled CdO + ZnO + α-Fe_2O_3 powder mixture with increasing milling time.

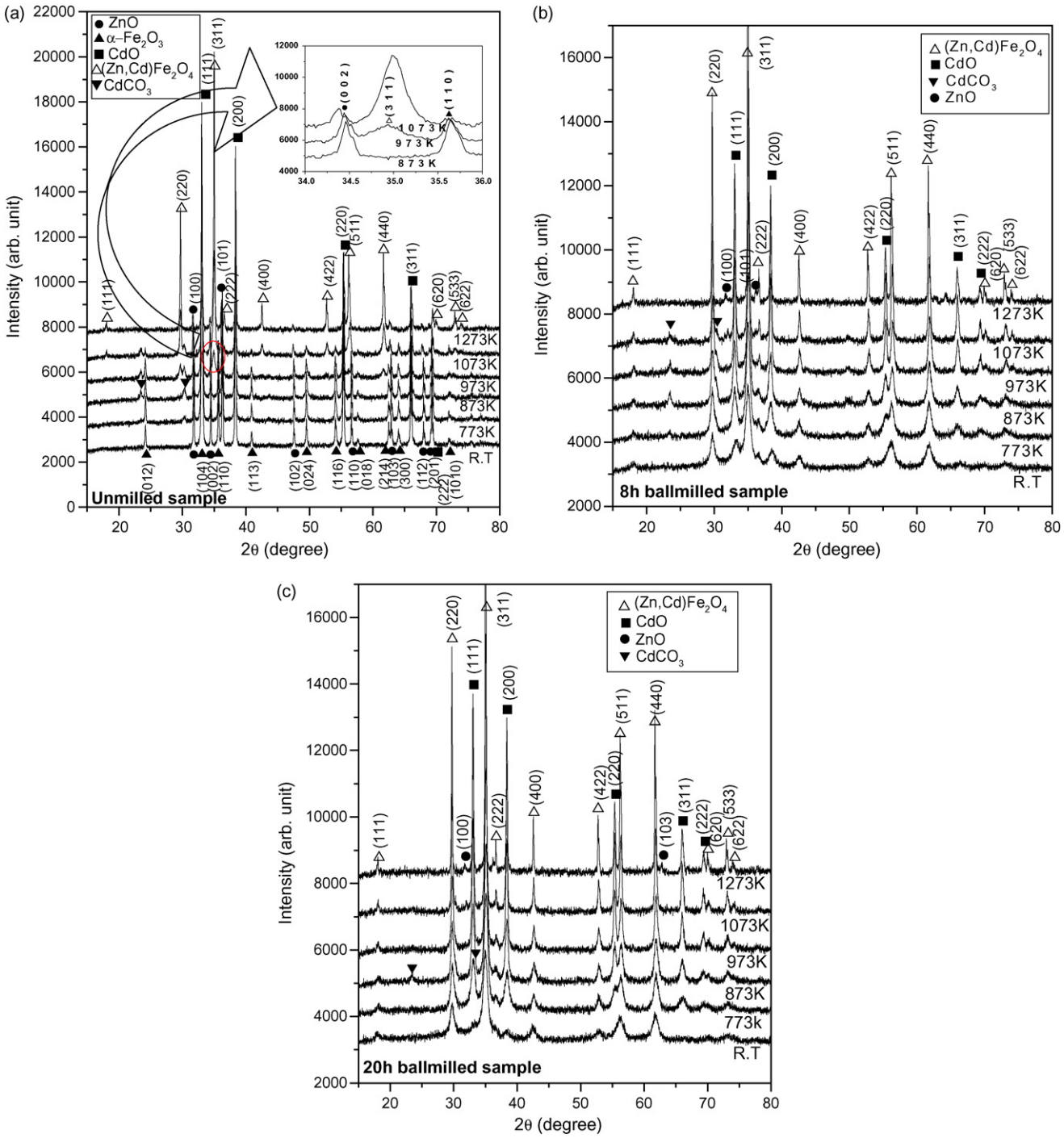

Fig. 6. XRD powder patterns of heat treatment of (a) unmilled, (b) 8 h ball-milled and (c) 20 h ball-milled samples at different elevated temperatures. The growth of the $(Zn,Cd)Fe_2O_4$ phase at temperature 973 K is shown in inset of (a).

decrease with increasing annealing temperature. At the initial stage of annealing, the CdO phase was transformed to $CdCO_3$ phase and its content increases up to 973 K and then decomposed into CdO and CO_2 phases. Therefore, the apparent decrease in CdO concentration after 773–1073 K can be attributed to the formation of $CdCO_3$ phase. At the annealing temperature 1273 K, the α-Fe_2O_3 phase content becomes zero but the CdO and ZnO phases still remain in the sample in an amount ~0.15 and ~0.07 mole fraction respectively. The ferrite phase content reaches ~0.77 mole fraction after annealing at 1273 K. It is obvious that the ferrite phase formed by sintering the stoichiometric powder mixture of CdO, ZnO and α-Fe_2O_3 is a non-stoichiometric Zn-rich ferrite phase. It can be noted in Fig. 6b and c that a small amount of CdO was also present in the ball-milled samples, and when the powders were annealed, the $CdCO_3$ phase formed, like in unmilled sample. If we ignore the presence of insignificant amount of $CdCO_3$ phase at the intermediate stages, then it can be observed that Fig. 7b and c are showing almost the same nature of variation. In both cases, initially the content of ferrite phase decreases with increasing annealing temperature by releasing the CdO phase only and this trend continues up to the annealing temperature 973 K. At higher annealing temperatures, the ZnO phase starts to leave the ferrite matrix but by this time the exclusion of ZnO phase is compensated to some extent by the inclusion of the CdO phase into the ferrite matrix and

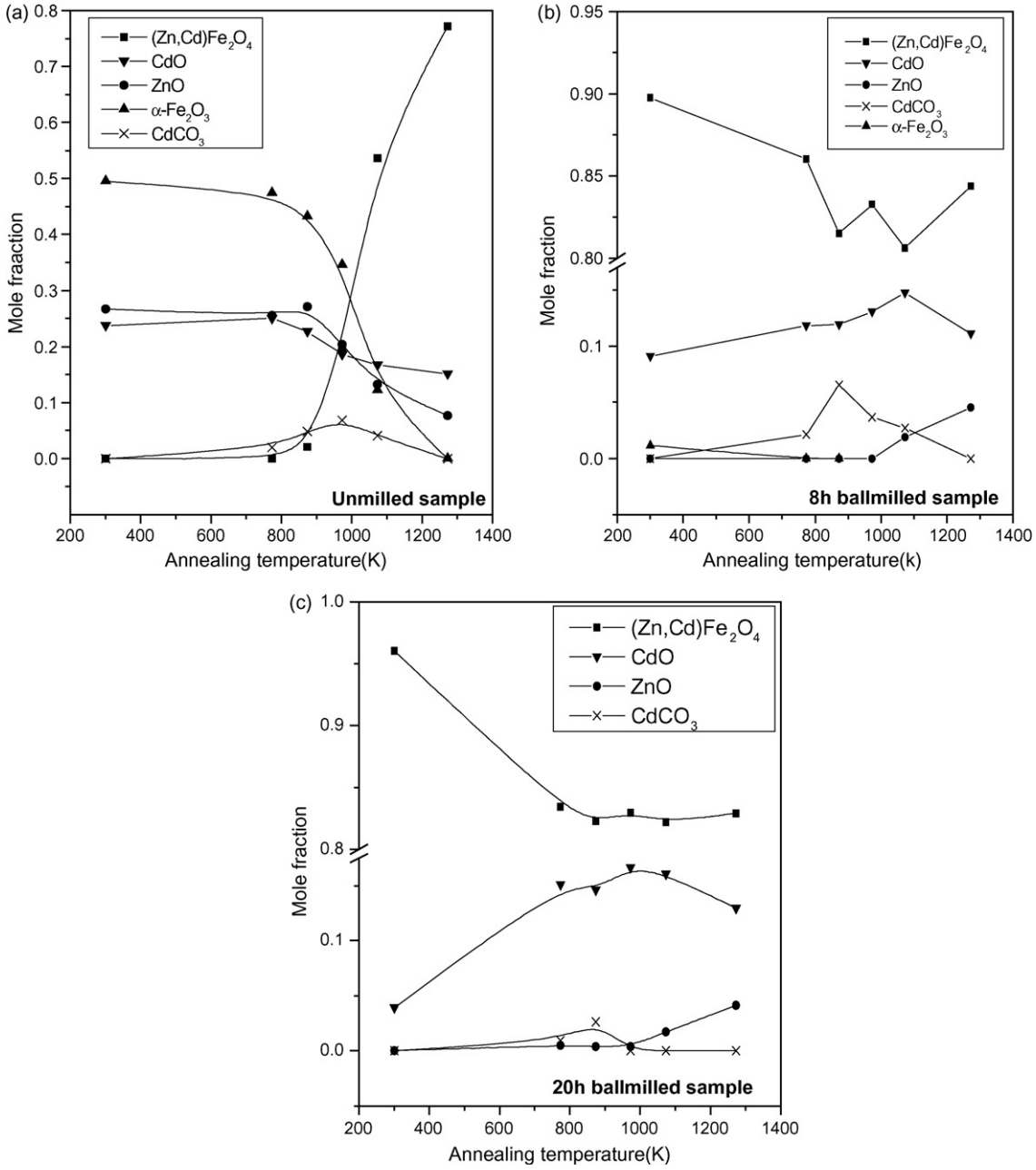

Fig. 7. Variation of mole fraction of different phases with increasing annealing temperature in (a) unmilled, (b) 8 h ball-milled and (c) 20 h ball-milled samples.

the ferrite phase content saturates at higher annealing temperatures. This nature of variations in CdO and ZnO contents clearly reveal that a Zn-rich ferrite phase formed at room temperature and remained stable up to 973 K and then slowly transforms towards a Cd-rich ferrite phase at higher annealing temperature. As can be seen from Fig. 6 that the α-Fe_2O_3 phase does not come out from the ferrite matrix even after annealing the sample at 1273 K, moreover, a small amount of α-Fe_2O_3 phase present initially in the 8 h ball-milled sample is absorbed in the ferrite phase during annealing. These observations led to the fact that by annealing the ball-milled samples it is not possible to get more stoichiometric ferrite phase, rather at elevated temperatures, one of the two divalent ions in the tetrahedral positions will dominate over the other.

Fig. 8 shows the nature of variation of lattice parameter of the ferrite phase for unmilled (0 h), 8 h and 20 h ball-milled samples. The ferrite phase in the unmilled mixture has grown with a high value (0.862 nm) of lattice parameter which is close to that of the Cd ferrite phase (0.869 nm). With increasing annealing temperature the lattice parameter value decreases and finally attains a value of 0.850 nm very close to Zn ferrite (0.844 nm) phase after annealing at 1273 K. The decrease of lattice parameter of the ferrite phase can be attributed to the substitution of Cd^{2+} ions of Shannon radius 0.84 Å by the Zn^{2+} ions of Shannon radius 0.60 Å at the tetrahedral positions [27]. For ball-milled samples the lattice parameter value decreases slightly up to 973 K and then increases slowly towards the lattice parameter value of unmilled sample at 1273 K. The initial decrease of lattice parameter up to 973 K is due to the release of Cd^{2+} ions from the ferrite lattice and formation of $CdCO_3$ phase, but at higher annealing temperatures $CdCO_3$ decomposes and Cd^{2+} ions diffuse into the ferrite matrix, the lattice parameter increases again. It may therefore be concluded that the compositions of the non-stoichiometric ferrite phase obtained by annealing the unmilled and ball-milled samples are almost equal.

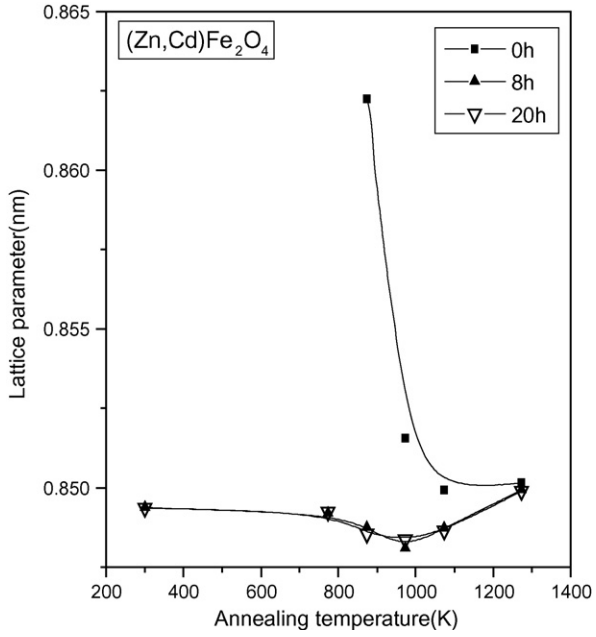

Fig. 8. Variation of lattice parameter of the ferrite phase in unmilled (0 h), 8 h ball-milled and 20 h ball-milled samples with increasing annealing temperature.

The nature of variation of particle size of the ferrite phase and the three starting phases with annealing temperature for the unmilled (0 h), 8 h and 20 h ball-milled samples are shown in Fig. 9a and b respectively. Fig. 9a shows that the particle size of the ferrite phase increases in all three (0 h, 8 h, 20 h) samples after annealing at 973 K with different rates. It is interesting to note that the particle size growth in unmilled (0 h) sample is much less than the ball-milled samples. The variation of particle size of the CdO, ZnO and α-Fe_2O_3 phases for the three samples are shown in Fig. 9b. In unmilled (0 h) sample particle size of CdO phase increases sharply up to 973 K and then the rate of increase becomes very slow and attains ~470 nm after annealing at 1273 K. In ball-milled samples, the CdO phase initiated with particle size ~5 nm at room temperature and increases continuously to ~238 nm and ~193 nm in case of 8 h and 20 h milled samples respectively after annealing samples at 1273 K. The particle size of the ZnO phase in unmilled (0 h) sample starts to increase after 773 K and after 973 K it saturates to a value ~230 nm. In case of ball-milled samples there is no effect of heating on the particle size. There is an initial increase in particle size of the α-Fe_2O_3 phase but very soon it saturates with increasing temperature to a value ~102 nm. From the variation of particle size of different phases with annealing temperature the variation of ferrite particle size in unmilled and ball-milled samples can be explained. In ball-milled samples the particle size of CdO phase increases at the final stage of milling but there is no change in ZnO particle size. In unmilled (0 h) sample, at the initial stage of annealing, particle sizes of CdO, ZnO and α-Fe_2O_3 phases increase very rapidly. Ferrite particles in unmilled (0 h) sample therefore grow in a constrained field at presence of larger particles of starting materials and the growth of ferrite particles at higher annealing temperatures was hindered to a great extend. In case of ball-milled samples ferrite particles grow in a comparatively free environment as the growth was not opposed that much by the smaller CdO and ZnO particles.

Fig. 10a and b depicts the variation of r.m.s. lattice strain of the ferrite phase and the other three starting phases respectively with increasing annealing temperature. The lattice strains of all phases are considered to be isotropic in nature. Fig. 10a shows that the lattice strain of the ferrite phase grown in unmilled (0 h) sample initially has a high value but decreases very rapidly with increasing temperature. But the lattice strain of the ferrite phase in ball-milled samples have much lower value initially in comparison to unmilled sample and decreases in a slow rate with increasing annealing temperature. The above observations are in full agreement with the observations on particle size variation of the samples with increasing annealing temperature. The growth of the ferrite phase in a constrained field in unmilled (0 h) sample is reflected in its initial high value of strain whereas, in ball-milled samples, the growth of the ferrite phase in a free environment is indicated by much

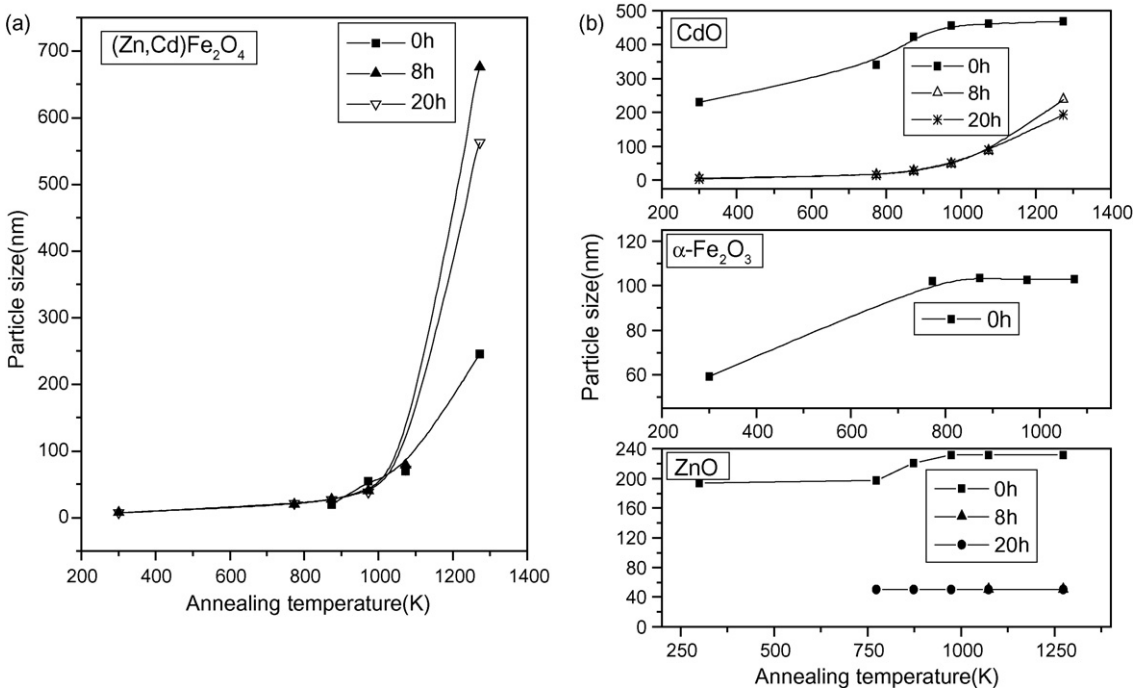

Fig. 9. Variation of particle size of (a) ferrite phase and (b) CdO, ZnO and α-Fe_2O_3 phases with increasing annealing temperature in unmilled (0 h), 8 h ball-milled and 20 h ball-milled samples.

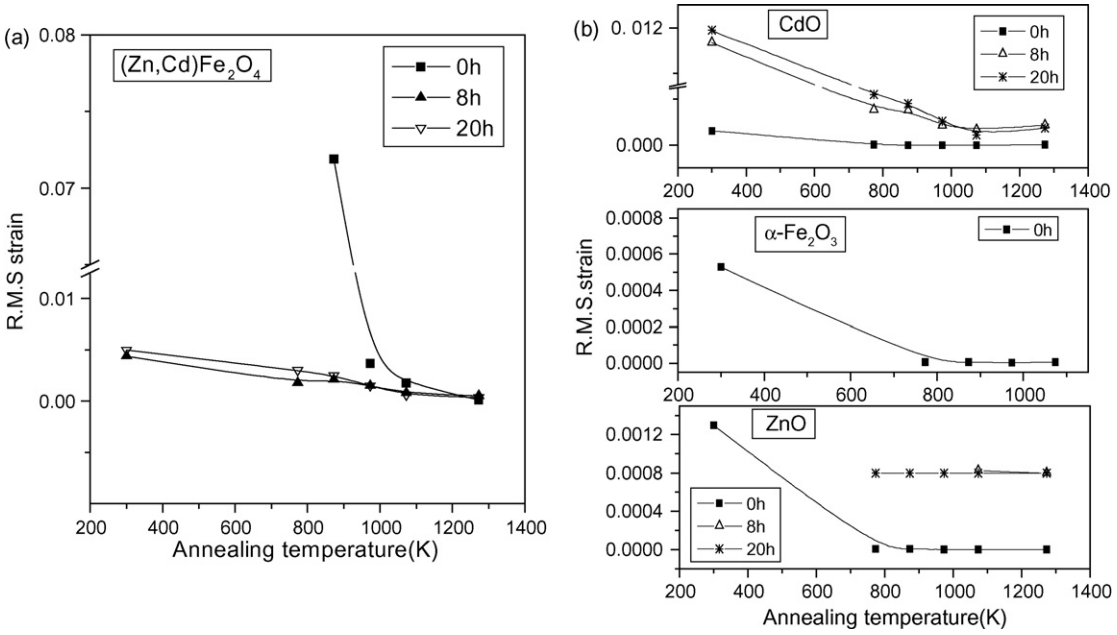

Fig. 10. Variation of r.m.s. lattice strain of (a) ferrite phase and (b) CdO, ZnO and α-Fe_2O_3 phases with increasing annealing temperature in unmilled (0 h), 8 h ball-milled and 20 h ball-milled samples.

lower initial value of lattice strain. Fig. 10b shows the variations of the lattice strain of CdO, α-Fe_2O_3 and ZnO phases with increasing annealing temperature. The room temperature value of lattice strain of CdO phase in unmilled (0 h) sample is very low and with increasing temperature initially there is a very small decrease up to 873 K and after that the lattice strain value saturates. In ball-milled samples the lattice strain value of the CdO phase is much higher initially and decreases rapidly with increasing temperature. The variations of lattice strain of α-Fe_2O_3 and ZnO phases in unmilled (0 h) sample have the same nature with increasing temperature. In both cases, lattice strains decrease up to 873 K and then saturate at higher temperatures. The lattice strain values of ZnO phase in ball-milled samples remain invariant with increasing temperature. These observations regarding the variations of lattice strain of the three starting phases are all in good agreement with the variations of particle size of the phases with increasing annealing temperature.

4. Conclusions

A stoichiometric mixture of CdO, ZnO and α-Fe_2O_3 powders subjected to high energy ball milling in air at room temperature up to 1 h milling results in formation of a non-stoichiometric Zn-rich (Zn,Cd)Fe_2O_4 phase with normal spinel structure with tetrahedral vacancies. After 25 h milling, 0.96 mole fraction of ferrite was formed and 0.04 mole fraction of CdO phase remained unreacted and particle size of ferrite phase reduces to ~7 nm. The phase stability and microstructure characterization of nanocrystalline (Zn,Cd)Fe_2O_4 powder annealed at elevated temperatures reveal that the Zn-rich ferrite phase remained stable up to 973 K and then slowly transformed towards Cd-rich (Cd,Zn)Fe_2O_4 phase following the release of divalent cations from ferrite lattice of normal spinel structure. The amount of ferrite phase decreases slowly with increasing annealing temperature. The ferrite phase has also obtained by conventional ceramic route by sintering the homogeneous stoichiometric mixture at 973 K for 1 h. The amount of ferrite phase increases continuously with increasing annealing temperature up to 1273 K. Like ball-milled ferrite phase, the sintered ferrite phase is also non-stoichiometric due to unreacted CdO phase. Particle size of ferrite phase in unmilled sample is quite small in comparison to ball-milled samples.

Acknowledgements

Authors wish to thank the University Grant Commission (UGC) India, for granting DSA–III programme under the thrust area “Condensed Matter Physics including Laser applications” to the Department of Physics Burdwan University under the financial assistance of which the work has been carried out.

References

[1] I. Anton, I.D. Dabata, L. Vekas, J. Magn. Magn. Mater. 85 (1990) 219.
[2] R.D. McMickael, R.D. Shull, L.J. Swartzendruber, L.H. Bennett, R.E. Watson, J. Magn. Magn. Mater. 111 (1992) 29.
[3] D.L. Leslie-Pelecky, R.D. Rieke, Chem. Mater. 8 (1996) 1770.
[4] T. Hirai, J. Kobayashi, I. Koasawa, Langmuir 15 (1999) 6291.
[5] R.H. Kodama, J. Magn. Magn. Mater. 200 (1999) 359.
[6] K.V.P.M. Shafi, Y. Koltypin, A. Gedanken, R. Prozorov, J. Balogh, J. Lendvai, I. Felner, J. Phys. Chem. 101B (1997) 6409.
[7] D. Niznansky, N. Viart, J.L. Renspinger, IEEE Trans. Magn. 30 (1994) 821.
[8] J.M. Yang, W.J. Tsuo, F.S. Yen, J. Solid State Chem. 145 (1999) 50.
[9] Y. Shi, J. Ding, X. Liu, J. Wang, J. Magn. Magn. Mater. 205 (1999) 249.
[10] P. Druska, U. Steinike, V. Sepelak, J. Solid State Chem. 146 (1999) 13.
[11] V. Sepelak, K. Tkacova, V.V. Boldyrev, U. Steinike, Mater. Sci. Forum 783 (1996) 228.
[12] V. Sepelak, A. Yu, U. Rogachev, D. Steinike, Chr. Uecker, S. Wibmann, K.D. Becker, Acta Crystallogr. Suppl. Issue A 52 (1996) C-367.
[13] V. Sepelak, A. Yu, U. Rogachev, D. Steinike, Chr. Uecker, F. Krumcich, S. Wibmann, K.D. Becker, Mater. Sci. Forum 139 (1997) 235.
[14] V. Sepelak, U. Steinike, D.Chr. Uecker, S. Wibmann, K.D. Becker, J. Solid State Chem. 135 (1998) 52.
[15] R.J. Hill, J.R. Craig, G.V. Gibs, Phys. Chem. Miner. 4 (1979) 317.
[16] C.P. Marshall, W.A. Dollase, Am. Miner. 69 (1984) 928.
[17] S. Bid, S.K. Pradhan, Mater. Chem. Phys. 82 (2003) 27.
[18] H. Dutta, M. Sinha, Y.C. Lee, S.K. Pradhan, Mater. Chem. Phys. 105 (2007) 31.
[19] M. Sinha, H. Dutta, S.K. Pradhan, Jpn. J. Appl. Phys. 47 (2008) 8667.
[20] H.M. Rietveld, Acta Cryst. 22 (1967) 151.
[21] H.M. Rietveld, J. Appl. Cryst. 2 (1969) 65.
[22] R.A. Young, in: R.A. Young (Ed.), The Rietveld Method, Oxford University Press, 1996, p. 1.
[23] L. Lutterotti, P. Scardi, P. Maistrelli, J. Appl. Crystallogr. 25 (1992) 459.
[24] L. Lutterotti, MAUD Version 2.046, 2006, http://www.ing.unitn.it/~luttero/maud.
[25] V. Sepelak, D. Schultze, F. Krumeich, U. Steinike, K.D. Becker, Solid State Ionics 141–142 (2001) 677.
[26] S. Bid, S.K. Pradhan, Jpn. J. Appl. Phys. 43 (2004) 5455.
[27] R.D. Shannon, Acta Cryst. A 32 (1976) 751.